Supplementary Data

Drug effect unveils inter-head cooperativity and strain-dependent ADP release in fast skeletal actomyosin

by

Nuria Albet-Torres[1*], Marieke J. Bloemink[2*] Tom Barman[3], Robin Candau[4], Kerstin Frölander[1], Michael A. Geeves[2], Kerstin Golker[1], Christian Herrmann[3,6], Corinne Lionne[3], Claudia Piperio[5], Stephan Schmitz[5], Claudia Veigel[5], Alf Månsson[1]

[1] Sch Pure Appl Nat Sci., University of Kalmar, SE-391 82 Kalmar, Sweden
[2]Department of Biosciences, University of Kent, Canterbury, Kent CT2 7NJ, UK
[3]UMR 5236, CNRS University of Montpellier I and II, France
[4] UMR 866 INRA University of Montpellier I, France
[5]NIMR, Mill Hill, London NW7 1AA, UK
[6]Present address: Physikalische Chimie 1,
Ruhr-Universitat Bochum, Universitat strasse 150, D-44780 Bochum, Germany

Supplementary Results

Supplementary Table 1. Percentage reduction in sliding velocity at pH 6.7 produced by 1 and 3 mM amrinone

	1 mM amrinone	3 mM amrinone
Experiment 1	18.8 %	21. 4 %
Experiment 2	17 %	32. 6 %
Experiment 3	49.1 %	-----

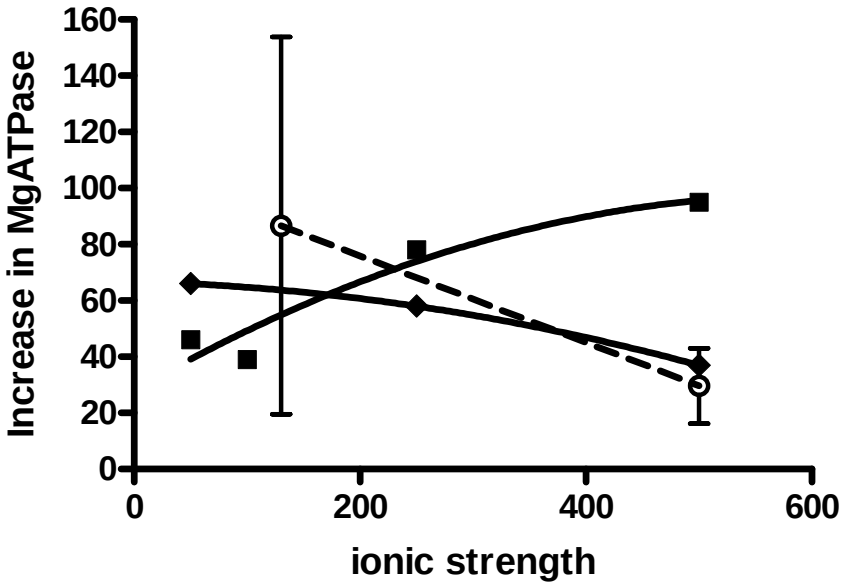

Supplementary Fig. 1. Percentage increase in basal MgATPase activity in response to 2 mM amrinone as a function of ionic strength of the assay solution. Dashed line and open circles: data from Fig. 2 in the main paper with 3 and 5 experiments at 130 and 500 mM ionic strength, respectively. Error bars: 95 % confidence interval. Filled symbols with associated fits to third degree polynomials: two other experiments with one given HMM preparation. Note experimental variability with no consistent effect of changes in ionic strength. However, as for the data in Fig. 2 of the main paper all results show a marked increase in MgATPase activity in the presence of amrinone.

Transient kinetic studies with chymotryptic S1 – interpretation and supplementary data

The progress curves of P_i production after mixing S1 with excess MgATP were biphasic: a P_i burst phase of amplitude A_{SS}, followed by a steady state rate, k_{ss} (Supplementary Fig. 2). During this latter phase, the rate constants of P_i and ADP release (k_4 and k_5 in scheme 1) direct catalytic activity (k_{cat}):

$$k_{cat} = \frac{k_0 \cdot k_5}{k_0 + k_5} \qquad (1)$$

where $k_0 = k_4 K_3/(1+K_3)$. The measured steady-state rate, k_{ss}, is proportional to k_{cat} and the fraction of active sites ([active site]):

$$k_{cat} = k_{ss\,/}\,[\text{active site}] \qquad (2)$$

In single-turnover experiments (*i.e.* [S1]>[ATP]; Supplementary Fig. 3) the progress curve of P_i production was described by a mono-exponential function. Again the P_i burst phase was too fast to be directly observed and only the P_i burst amplitude (A_{STO}) could be evaluated. In the single-turnover experiments the burst amplitude depends on equilibrium constant of the cleavage step (K_3 in scheme 1), *i.e.*, it is independent of active site concentration:

$$A_{STO} = K_3/(1+K_3) \qquad (3)$$

In the same line, the observed rate constant (k_0) is independent of active site concentration being directed by k_4 and K_3:

$$k_0 = k_4 K_3/(1+K_3) \qquad (4)$$

On basis of the results in Supplementary Figs. 2 and 3 and, using equations (1) – (4), the effects of 2 mM amrinone on the constants k_{cat}, k_4, k_5 and K_3 could be deduced as summarized in Supplementary Table 2.

Supplementary Table 2. Multi and single-turnover P_i burst experiments performed at 4°C to assess the effect of amrinone on S1 ATPase activity and individual steps. In single turnover P_i time course, the reaction mixture was 10 µM S1 + 1 µM [γ^{-32}P]ATP ± 2 mM amrinone. The evaluation of equilibrium constant of cleavage step (K_3) and rate constants of P_i and ADP release steps was obtained from the combination of the two types of experiment.

Constant	- AMR	+ AMR	
K_3	2.23	2.31	
$k_o = k_4K_3/(1+K_3)$	0.06 s^{-1}	0.075 s^{-1}	
k_4 (P_i release)	0.087 s^{-1}	0.108 s^{-1}	from STO
k_{SS}	0.010 s^{-1}	0.0135 s^{-1}	
A_{SS}	0.54	0.49	
[Active site] $(A_{SS} \times (1+K_3)/K_3)$	0.78	0.70	
k_{cat}	0.0128 s^{-1}	0.0193 s^{-1}	
k_5 (ADP release)	0.0163 s^{-1}	0.0260 s^{-1}	

STO = single turnover condition; $k_o = k_4K_3/(1+K_3)$; $k_4 = P_i$ release rate constant ; k_5 = rate constant of the isomerization step before ADP release (diffusion limited); k_{cat} = catalytic activity of S1.

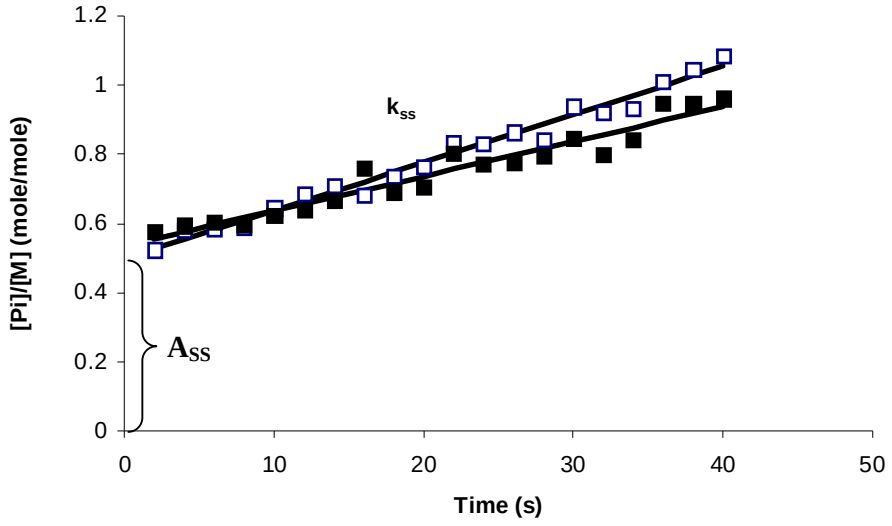

Supplementary Fig 2. Rapid quench flow experiments under multi-turnover conditions. P_i time course with S1 at 4 °C. Reaction mixture was 3 µM S1, 12 µM [γ^{-32}P]ATP ± 2 mM amrinone. $k_{ss} = k_{cat}$ [active site]. $A_{SS} = \frac{[\text{active} - \text{site}] \cdot K_3}{1 + K_3}$; M = myosin head (S1) concentration; ■ without AMR; □ with AMR. For kinetic constants see Supplementary Table 2.

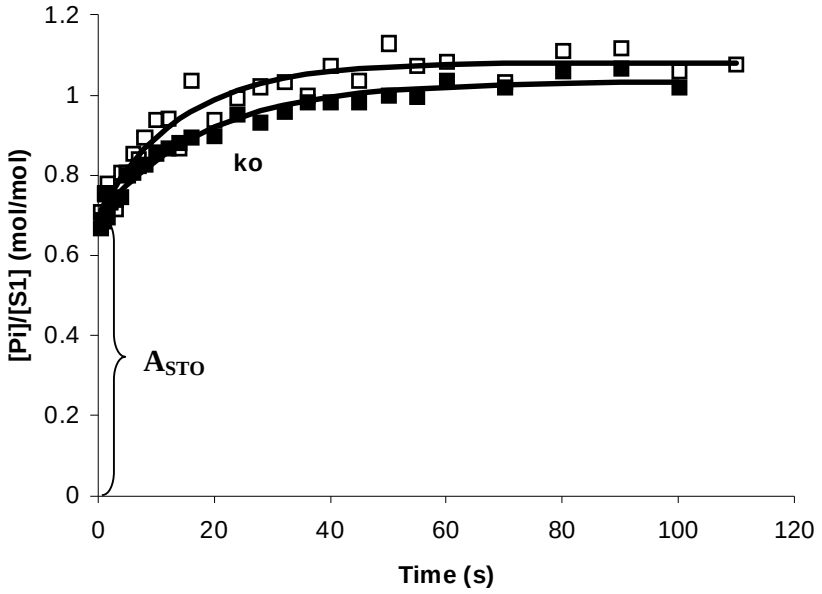

Supplementary Fig. 3. Single turnover P_i time course with S1 at 4 °C. Reaction mixture was 10 µM S1, 1 µM [γ^{-32}P]ATP ± 2 mM amrinone); $k_0 = k_4 K_3/(1+K_3)$; $A_{STO} = K_3/(1+K_3)$.
■ = -AMR; □= +AMR

Supplementary Discussion

Methodological considerations related to amrinone effects on different myosin isoforms and muscle cells

A majority of the *in vitro* motility assay experiments, as well as the steady-state myosin MgATPase assays, in the present study, were performed using fast leg muscle from the rabbit in order to facilitate comparison with earlier *in vitro* motility assay studies (2). However, since the fast leg muscle myosin contains a mixture of the heavy chain isoforms IIx/IId and IIb (2), all transient kinetic and optical tweezers studies were performed using myosin from rabbit *psoas* muscles. Since this muscle is known to be entirely dominated by a single myosin isoform (heavy chain IIx/IId) (3) interpretation of the data is simplified. The present experiments were performed in four different labs and, for practical reasons, the standard experimental conditions of each lab were used. As a consequence, there was some difference in buffer composition and ionic strengths between different types of experiments.

Importantly, there are several lines of evidence to suggest that these differences are not of any critical importance, *e.g.* they would not prevent us to interpret the data within one general framework. First, similar effects of amrinone were demonstrated in the *in vitro* motility assay with varying experimental conditions, as regards ionic strength, pH, temperature and the biological buffer system (MOPS or Imidazole (2)). Second, whereas the effect of amrinone on the HMM induced sliding velocity was slightly lower with *psoas* HMM, the difference from HMM of leg muscle was marginal at nearly physiological temperature. Third, similar effects of amrinone on actomyosin function have been demonstrated using fast skeletal muscle myosin or muscle preparations from several sources and with experiments performed under different conditions in different labs. These previous studies with similar results, include intact skeletal muscle fibers of the frog (4), intact toe muscles of the mouse (5), skinned muscle fibres from rat *psoas (6)* and, finally, HMM from fast rabbit leg muscles (2). All these earlier studies, using fast myosin or fast muscle fibers, detected quantitative effects of 1 – 3 mM amrinone on sliding speed/unloaded shortening velocity, that were remarkably similar (average 25 – 33 % reduction) and also very similar to the effects observed here. In contrast, there were only small effects (~10 %) on the unloaded shortening speed of slow skeletal muscle fibers of the rat (6).

The possibility has been considered (7) that the critical rate constant determining shortening velocity of fast skeletal muscle switches from k'_5 or k'_6 at close to physiological temperatures to k'_2 at lower temperatures (*e.g.* below 25 ^{o}C). If amrinone reduces sliding velocity by affecting one of the mentioned rate constants there may be quantitatively different effects of the drug at temperatures below 25 ^{o}C and at temperatures close to 30 ^{o}C (used in a majority of the present *in vitro* motility assays). We tested this by comparing motility assay results at 23 ^{o}C and 29 ^{o}C (Table 1, main paper). Lower temperatures were not used since, at least one study (8) has shown substantial differences in the temperature dependence of *in vitro* sliding velocities and the unloaded shortening speed of muscle cells at temperatures just below 20 ^{o}C.

Binding site of amrinone

The unique effects of amrinone on the force-velocity relationship form the basis for deeper insight into the mechanisms underlying this relationship if the kinetic effects of amrinone on actomyosin are characterized on the molecular level. As pointed out in the main paper, this does not rely on knowledge of the exact binding site(s) of amrinone on the myosin head. Efforts to gain such knowledge were therefore outside the scope of the present work. Moreover, the required experiments would have been highly challenging with limited chances for success due to *e.g.*: 1. low solubility of the drug coupled to low affinity for actomyosin and 2. intense amrinone fluorescence in the UV-region.

The low solubility and low affinity makes it highly challenging to crystallize myosin together with the drug for subsequent structure determination by X-ray diffraction. The intense fluorescence, on the other hand makes it impossible to use tryptophan fluorescence for monitoring structural changes related to amrinone binding. However, in view of the unique combination of effects of amrinone on the force-velocity relationship, it may be regarded of interest in the future to clarify the exact binding site. We believe that this may be achieved by studying drug effects on genetically modified myosin, engineered to lack certain specific amino acids or domains that are suspected to bind amrinone. This indirect method would provide candidate binding sites in the myosin head which may then be corroborated *e.g.* by molecular dynamics simulations of amrinone docking to the appropriate domain. Not only the location of the binding site(s) for the drug but also the number of such sites is difficult to establish. We performed equilibrium dialysis studies to estimate this number for S1 (in the absence of actin; data not shown). It was not possible to obtain conclusive results since the highest amrinone concentration that could be readily evaluated in these studies was 200 μM. However, the results suggested a dissociation constant of amrinone of almost 1 mM and no evidence for a site with dissociation constant in the range of 0.2 mM, or below, could be found. As further discussed below, other experimental results are consistent with one binding

site as the basis for the amrinone effects but the possibility of two sites cannot be fully excluded.

In accordance with earlier results for CaATPase (6) and basal MgATPase activity (2), amrinone moderately increased the MgATPase of myosin and HMM in the absence of actin, suggesting that the drug increases the rate constant k_4 (Scheme 1). Neither this effect nor the reduction in K_{AD} was observed with S1. This is in contrast to the increased rate of MgATP-induced dissociation seen both with myosin, HMM and S1. The latter effect saturated at lower concentration (0.1 – 0.2 mM) than those on the basal MgATPase activity, sliding velocity (2) and K_{AD} ([amrinone] > 0.5 mM). In view of these results it is tempting to speculate that amrinone binds to two different sites. However, the equilibrium dialysis experiments with S1 (in the absence of actin; see above) gave a dissociation constant > 0.5 mM. This suggests that the difference in concentration dependence may be attributed to higher drug affinity in the absence of MgADP and the presence of actin (as under conditions when $K'_1k'_2$ is measured), rather than to the binding to two different sites. Moreover, effects on sliding velocity may require cooperativity between HMM molecules with binding of the drug to a substantial fraction of the myosin heads to become apparent. This is clear from motility assays where inhibited and uninhibited myosin motors are mixed (9). With regard to the *combination* of increased basal myosin MgATPase and reduced sliding velocity, this has been observed previously for several point mutations within the myosin motor domain (*e.g.* in switch II and the SH1 and SH2 helices) (10-12), and also using a fluorescent ATP analogue (Alexa-ATP) (13). This is compatible with the idea that also the effects on MgATPase activity, sliding velocity and K_{AD} could be ascribed to a drug binding site in the motor domain. Within this framework, the lack of amrinone effect on the MgATPase of chymotryptic S1 can be interpreted to mean that drug effects are propagated to the regulatory light chains and that this region needs to be intact in order for the effect on MgATPase activity to become apparent. Alternatively, amrinone actually requires two heads to exert its actions on the MgATPase.

The MgATP turnover rate may be slightly inhibited by temporary head-head interactions in the absence of drug (14) and the possibility exists that drug binding reduces these interactions. Such an effect is not far-fetched considering effects of another drug, blebbistatin on, head-head interactions. The latter drug binds in the motor domain close to switch II (15).

The discussion above suggests that it is unlikely that the effect on the MgADP-affinity is due to binding of amrinone to another site than the effect on MgATP induced detachment rate. However, for the sake of completeness it may be relevant to consider possible reasons why HMM could exhibit one additional site (per head) than S1. First, if the presence of two heads causes structural changes in the motor domain, a new site may become available in this region. Alternatively, the extra site may be located in a region that is present neither in chymotryptic S1 nor in papain S1. One candidate region would be the immediate neighborhood of the light chains. However, if this is the case, it is surprising that the effect of amrinone on MgADP affinity in acto-HMM is absent in *both* chymotryptic S1 and papain S1. Thus, the first fragment has intact essential light chains and the second fragment intact regulatory light chains. The finding that the sliding velocity of S1-propelled actin was reversibly reduced by amrinone is also difficult to reconcile with the idea that the binding site responsible for the effect on MgADP affinity is present only in two-headed myosin fragments. Thus, although the effect on sliding velocity was considerably smaller with S1 than with HMM, the effect cannot be explained by the amrinone induced increase of the MgATP induced detachment rate. This effect would have increased the velocity. The smaller reduction of velocity with S1 may be attributed to adsorption of the S1 fragments to the surface via the regulatory light chain regions. Clearly, even if the drug binds to a single site in the motor domain, the light chain region may be important for the drug effects, particularly since they appear to involve strain dependent mechanisms.

In spite of the above arguments, the possibility of two binding sites for amrinone cannot be fully excluded. If we accept the idea that amrinone exerts its actions on the MgATP induced detachment rate by another mechanism than the effects on basal MgATPase and MgADP affinity (only seen in HMM) it is of interest to consider the consequences in terms of molecular interpretations.

First, if the increased MgATP induced detachment rate would be explained by a separate mechanism, either of the two alternative explanations considered below (increase of free energy of state A_2 or reduction of free energy of state A_1) for the amrinone actions on velocity and MgADP affinity would be equally likely. Indeed the stabilization of the A_1 state would gain in likelihood since it would be more readily consistent with the increased basal MgATPase activity if also the M* ADP state in HMM is stabilized by amrinone.
If an additional drug binding site is available in HMM, one may also consider the possibility that amrinone reduces the rate constant k'_6 rather than the rate constant k'_5. However, there have been recent doubts whether k'_6 is sufficiently slow to limit shortening velocity (7). Moreover, it seems unlikely that amrinone would affect such a simple process as diffusion of MgADP away from an open active site pocket and that this effect would appear in HMM and not in S1. It seems more likely that a drug would affect the more complex structural change that opens the active site pocket, *e.g.* by effects on k'_5.

The detailed mechanism by which amrinone exerts its actions may be deciphered by transient kinetics studies such as displacement of MgADP from the active site of acto-HMM and acto-S1 by saturating concentrations of MgATP. Whereas an effect of amrinone on k'_6 would be expected to appear both in S1 and HMM (provided that the drug binds to both fragments) effects on k'_5 would be possible to probe only in acto-HMM (16). The reason is that the AM*ADP state would be substantially populated in solution only with two-headed myosin

fragments. In this case one would expect a double exponential actomyosin detachment upon addition of a saturating MgATP concentration in the presence of MgADP. Here, the fast phase would represent detachment of heads in the AM ADP state (corresponding to trailing heads), which have their light chain binding region strained in a way to oppose shortening during active contraction. The slow phase, on the other hand, would represent detachment of the oppositely strained AM*ADP partner heads of each HMM molecule (16). If amrinone affects k'_5 in HMM, rather than k'_6, one would expect that the drug has no effect on the fast exponential rate (about 300 s^{-1} at 12 ^oC and similar to that with S1). However, one would expect increased relative amplitude of the slow phase at the expense of the fast phase. Additionally, the rate of the slow phase would be reduced.

Indeed, preliminary experiments provided very clear evidence supporting the view that amrinone affects k'_5 rather than k'_6. Thus, whereas 1 mM amrinone did not effect the rate of the fast phase, the drug reduced the relative amplitude of this phase by almost 50 %. This occurred with a compensatory increase in the relative amplitude of slow phases. However, in contrast to the simple model, there were two slow phases, rather than one, and the amplitude of both phases was increased by 1 mM amrinone whereas the rates of both were reduced by about 40 %. Due to the complexity with three phases, a detailed analysis is outside the scope of the present study and we are presently investigating the phenomenon in greater detail.

In summary, the above arguments suggest that amrinone exerts its actions by binding to one given site. Differences in concentration dependence for different effects may be readily explained. They are likely to reflect either different affinity for amrinone in different myosin/actomyosin states or, as in the case of *e.g. in vitro* motility assays, the apparent concentration dependence may be influenced by cooperative effects between myosin molecules. However, whereas the possibility seems unlikely, we can presently not fully

exclude that amrinone exerts its actions by binding to two sites. Importantly, however, the above discussion suggests that even if amrinone would exert its actions by binding to two sites this does not change the major conclusions of the paper. Thus, the only observed effect of amrinone that could possibly account for the reduction of the sliding velocity is the increased MgADP affinity. Above, we provide evidence that this effect is likely to be due to a reduction of k'_5 whether or not it is attributed to binding to another site than that underlying the effect on the MgATP induced detachment rate. Finally, the fact that an effect on k'_5 also simulates the effects of amrinone on the force-velocity data is further support of the explanation.

Supplementary Theory

Modification of the statistical model of Edman *et al.* (1997).

The cross-bridge cycle in the model of Edman *et al. (17)* includes 4 different states according to the kinetic scheme in Supplementary Fig. 4 A. The free energy diagrams of these states, as a function of the distance (x) between a reference position on myosin and the nearest myosin binding site on actin, are illustrated in Supplementary Fig. 4 B (see also Fig. 9 of main paper). The value of x = 0 nm is here defined as the position of the myosin head relative to the actin site where force is zero in state A_2. The rate constants (or rather rate functions depending on x and v) for transitions between different states of the model are given in the Supplementary Fig. 4 C – F. These rate functions are thermodynamically consistent with the free energy diagrams in Supplementary Fig. 4 B. In both the original model of Edman *et al.*, and the modified model developed here, the two heads of one myosin molecule are assumed to be independent. Furthermore, each head is only assumed to be within reach of one binding site on actin. It is important to note that the absolute values of the rate functions in Supplementary Fig. 4 C - F are adapted to fit data of fast frog muscle fibers at low temperature, *e.g*. Fig. 1 of main paper. Initially, we made attempts to simulate the amrinone effects on the force-velocity

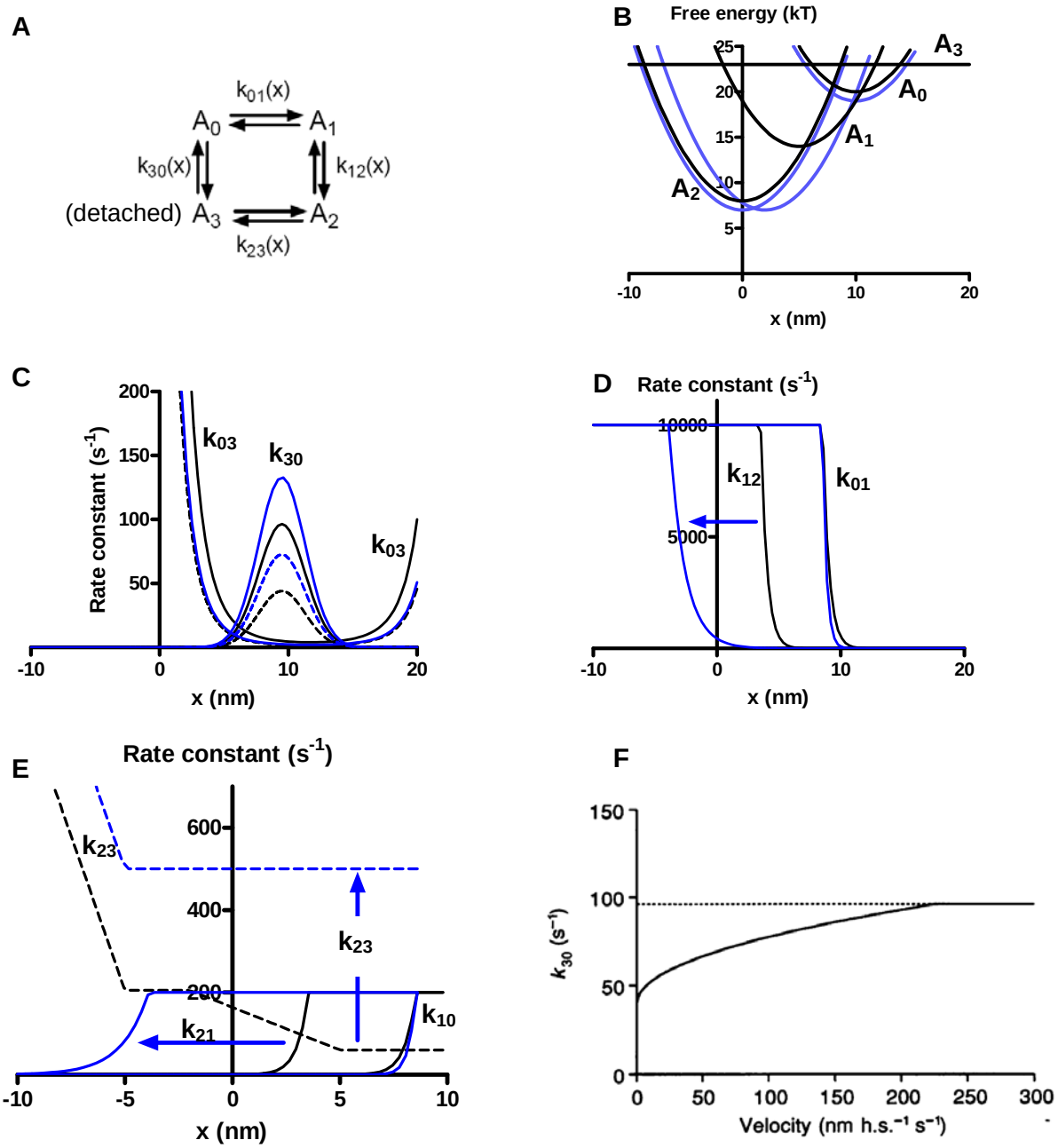

Supplementary Fig. 4. Overview of model of Edman *et al.*[9] and modified version of this model (blue) used for simulations in the main paper. (A). Kinetic scheme describing original cross-bridge model. The free energies of the states A_0 – A_3, and thereby, the rate constants for the transitions between them depend on the relative position (x) of the myosin head and the actin site. (B). Free energy diagrams for the different states in A, in the original model of Edman *et al.* (black), and in the modified model (blue lines). (C). Attachment rate functions (depend on x and v) for transitions from state A_3 into state A_0 and the inverse of these rate functions (reversible attachment). Black and blue lines represent original and modified model, respectively. Full lines represent rate functions at high velocity whereas dashed lines represent rate functions at close to zero velocity. The velocity dependence is described in Suppl. Fig. 4 F. (D). Forward rate functions $k_{01}(x)$ and $k_{12}(x)$. Main change in modified version of the model compared to original model illustrated by blue arrow and blue lines. (E). Reverse rate functions $k_{10}(x)$ and $k_{21}(x)$ (filled lines) and detachment rate function $k_{23}(x)$, (dashed line). Main modification of model compared to model of Edman *et al.* indicated by blue arrows and lines. (F). Velocity dependence of attachment rate function k_{30}. Velocity dependence illustrated only for the original model of Edman *et al.* and for the maximum value (peak of Gaussians in C) of this rate function. Similar velocity dependence in modified model but different absolute values of highest and lowest value of $k_{30}(x, v)$ according to Suppl. Fig. 4 C.

relationship by using the original model of Edman *et al.* First, we reduced the rate constant for dissociation of myosin heads from the state A_2 (50 % reduction for all values of x). Whereas this change gave a roughly 50 % reduction in the sliding velocity (Supplementary Fig. 5) and a reduced curvature of the force-velocity relationship at low loads (< 80 % of maximum force) there were only minor effects on the maximum isometric force. However, most importantly, there was a very poor fit of the model to the high-force region of the force-velocity relationship. We next attempted to simulate the amrinone effects by leaving the dissociation constant from the state A_2 unaltered, instead assuming that amrinone stabilized the state A_1. This was achieved in the model by shifting the free-energy curve for the state A_1 downwards by 2 kT, without any other modifications. The resulting changes in the rate functions led to a substantial increase in the isometric force (considerably larger than seen experimentally) and a substantially reduced deviation of the force-velocity relationship from the hyperbolic shape in the high-force region (Supplementary Fig.5). However, there was an increased curvature (rather than decreased as observed experimentally) of the force-velocity relationship in the low-force region and only a very small reduction in maximum sliding velocity.

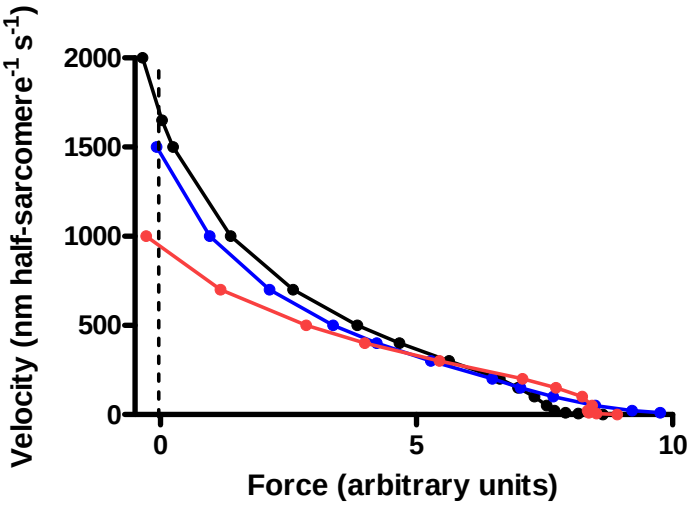

Supplementary Fig. 5. Attempts to simulate the effects of amrinone by using the original model of Edman *et al* (9). Black symbols represent the control condition and were simulated using the original parameter values of Edman *et al*. The red symbols represent attempt to simulate amrinone effect by reduced rate constant of detachment from the state A_2. The blue symbols represent attempt to simulate amrinone effects by shifting the free-energy profile of state A_1 downwards without other effects. Vertical dashed line represents zero load (force). Data points connected by lines to simplify viewing.

Supplementary Fig. 4 B – E show how the model of Edman *et al.* was modified (blue lines) in a way that the different states could be more readily identified with their biochemical equivalents in scheme 1 of the main paper. To achieve this, we shifted the free energy diagram for the state A_1 both downwards and to the left. By changing the model in this way there were changes in important rate functions and we made the model more similar to that of Duke (18,19). It then became natural to associate the states A_0 and A_1 with the AM ADP P_i and AM* ADP states, respectively. Moreover, the AM ADP, AM and AM ATP states could be lumped together into the state A_2 and the states with myosin dissociated from actin into the state A_3. In modifying the model of Edman *et al*. it was important to make sure that it still fitted the force-velocity data in the absence of amrinone. To ensure this, the shifts of the free-energy diagram of state A_1 were accompanied by small downward shifts of the free energy of states A_0 and A_2 (Supplementary Fig. 4 B) with resulting changes in associated rate constants, *e.g*. increase of the attachment rate constants (Supplementary Fig. 4 C). Moreover, the rate constant for dissociation from state A_2 was increased as indicated in Supplementary Fig. 4 E to give a reasonable sliding velocity in the control situation.

Commented Simnon^{TM} source code for the simulations are given below. The commented version of the model is that of Edman *et al.* (17). However, this version differs from the presently modified model only in the choice of parameter values.

The lumping together of the chemical states AM ADP, AM and AM ATP into the model state A_2 requires some justification. Whereas the free-energy minima of the states AM ADP and AM are likely to differ by about 2 kT at physiological MgADP concentrations (20) we assume that they have their free-energy minimum at the same value of x. This assumption, which is similar to that of Pate and Cooke (20) , gains support from the lack of structural changes in actin-attached skeletal S1 upon binding of MgADP (see references main paper).

Under these conditions it is justified to lump the two states together since a transition from the AM ADP to the AM state would not change the force developed. The latter is given by the slope, dG/dx, of the free energy diagram. This slope would be the same for the AM and AM ADP states at each value of x if the free-energy diagrams are only displaced vertically. However, it is clear that by lumping together the states AM ADP, AM and AM ATP the rate function k_{23} (x) is affected by the transition between all these states as well as by the actual dissociation step between actin and M ATP. It is straightforward to show that k_{23} (0) (*i.e.* the value of k_{23}(x) for the free energy minimum of the state A_2) can be written as follows, using the terminology in scheme 1 in the main paper:

$$k_{23} = \frac{k'_2[\mathrm{MgATP}]}{\frac{k'_2}{k'_6}[\mathrm{MgATP}] + \frac{1}{K'_1} + [\mathrm{MgATP}]} \qquad (5)$$

This expression applies to the physiological conditions in a muscle cell with low concentration of MgADP.

Simulation of amrinone effects using modified model of Edman *et al.*

In the main paper we probed all parameters (fraction of weakly bound actomyosin states, myosin step length, rate of MgATP induced dissociation and rate of MgADP release by actomyosin) that have been proposed to determine the sliding velocity of skeletal muscle fibers. Our results show that the reduction in a strain-dependent rate constant of MgADP release is the only observed effect of amrinone that may account for the reduced sliding velocity caused by the drug. In terms of the modified model of Edman *et al.* (Supplementary Fig. 4) such an effect could either correspond to a stabilization of the state A_1 (AM* ADP-state; lowering its free energy compared to the other states) or to a weakening of the actomyosin affinity in the A_2-state (increase of its free energy compared to the other states). In order to simulate the amrinone effects on the force-velocity relationship it is also necessary to include the effects of the drug on the MgATP induced dissociation of actomyosin. For the

latter purpose we assume (on basis of myofibril data; main paper) that K'_1 is reduced by amrinone by 50 % whereas k'_2 is increased by 80 % by the drug. In different studies, either k'_2 or k'_6 have been assumed to be rate limiting for dissociation from the state corresponding to A_2 (7,21,22). Whether k'_2 or k'_6 is rate limiting could also depend on the exact temperature, the ionic strength and the species from which the skeletal muscle myosin is isolated (7,22). The uncertainties in the literature data could indicate that k'_2 and k'_6 are quantitatively rather similar. However, if instead, $k'_6 << k'_2$ it is evident from equation 5 that the amrinone induced changes in k_2 would have negligible effects on the rate constant k_{23}. If $k'_2 \approx k'_6$, then k_{23} would be increased by 20 % by the combined effects of amrinone on K'_1 and k'_2. Finally if $k'_2 << k'_6$ and [MgATP] ≈ 5 mM (as *in vivo*), k_{23} would be increased by about 60 % by amrinone.

As mentioned above, the reduction in the rate constant of the strain dependent MgADP release could be explained either by reduced free energy of the state A_1 or increased free energy of the state A_2. In terms of the modified model of Edman *et al.* both mechanisms account for the observed effects of amrinone on the force-velocity relationship of skeletal muscle (see main paper and below). However, increased free energy of the state A_2 seems most likely since such an effect would be consistent with both a reduction of k'_5 and an increase of k'_2 in the kinetic scheme 1 (main paper). This is clear since the difference in free energy between two states is proportional to $-\ln(k_{ij}/k_{ji})$ where k_{ij} and k_{ji} are the forward and backward rate constants for the transition between the two states. Thus, an increase of the free energy of state A_2 without changes in the free energy of any other state would be in line with both a reduction of k'_5 and an increase of k'_2 in scheme 1 (main paper). Simulations of the amrinone effects on the force-velocity relationship of skeletal muscle on basis of an increased free energy of state A_2 are illustrated in Fig. 10 B-C in the main paper. In that simulation it is assumed that $k'_6 << k'_2$. As a result (Eq. 5), the effects of amrinone on k'_2 and K'_1 do not affect the rate function $k_{23}(x)$ in the model. In the simulation in Supplementary Fig. 6 A it is

instead assumed that $k'_2 << k'_6$ whereas all other parameter values are the same as in the simulations in 10 B in the main paper. In this case, $k_{23}(x)$ is determined largely by k'_2 and the amrinone-effects on this rate function will have noticeable effect in addition to the effect of a reduction in k'_5. It can be seen in Supplementary Fig. 6 A that the change in free energy of state A_2 in the model can account quite well for the high-force region of the experimental force-velocity data whereas the simulated maximum sliding velocity is considerably higher than observed experimentally. The latter discrepancy can be amended by a further increase (2 kT instead of 1.3 kT higher than in the control solution) of the free energy of the state A_2. Thus, as can be seen in Supplementary Fig. 6 B, a 60 % increase in $k_{23}(0)$ in response to amrinone in combination with a 2 kT increase in free energy of the state A_2 accounts well for the amrinone induced reduction in sliding velocity. However, in this case there is a poor fit of the model to force-velocity data at intermediate forces.

The above simulations, together with those in Fig. 10 in the main paper, show that the amrinone effects are most readily modeled by an increase of the free energy of state A_2, leading to a reduction of the rate function $k_{12}(x)$ (corresponding to k'_5 in scheme 1 of the main paper) but only negligible effects on the rate function $k_{23}(x)$. This accords with the idea that $k'_6 << k'_2$.

As mentioned in the main paper, it is clear that the amrinone effects on the force-velocity relationship and the reduced rate of a strain-dependent MgADP release may also be modeled by a decrease in free energy of the state A_1. The changes in the free energy diagrams and in

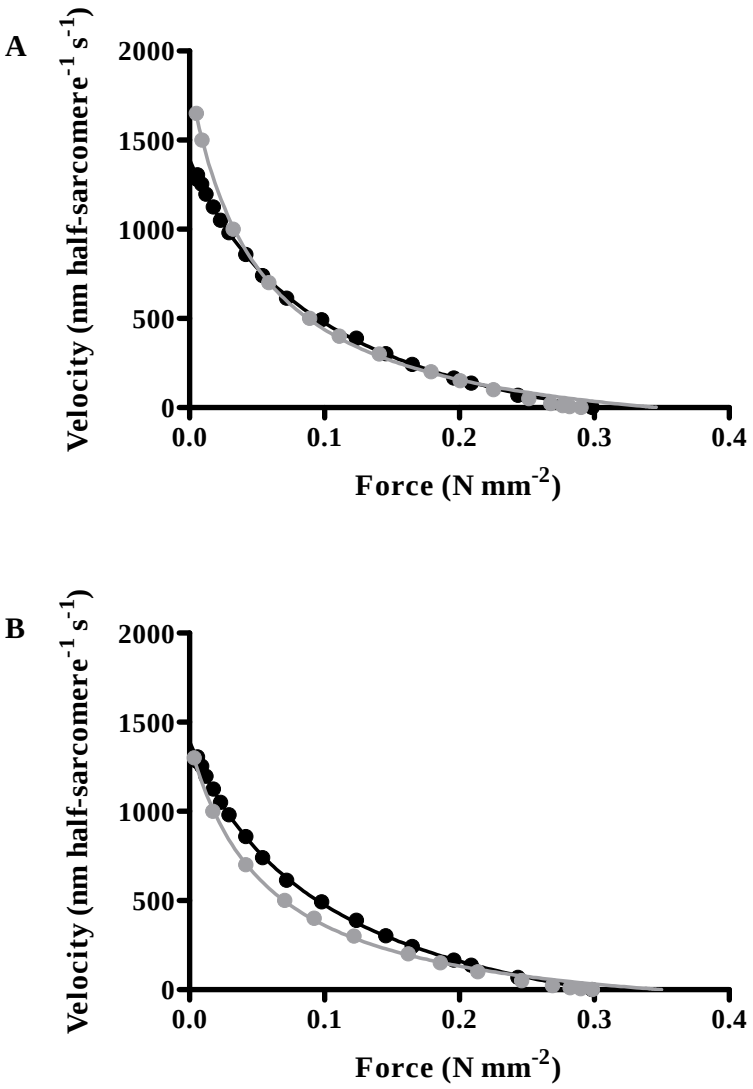

Supplementary Fig. 6. **Simulation of amrinone effects on force-velocity relationship assuming increase of k_{23} and increased free energy of state A_2.** (A). Simulated force-velocity data (grey circles) superimposed on the experimental amrinone data from Fig. 1 of main paper (black circles). Amrinone data simulated by the following changes from the control conditions (main paper; Figs. 9 and 10A): increase of free energy of state A_2 by 1.3 kT and increase of rate function $k_{23}(x)$ by 60 % for x > -5 nm. Both simulated and experimental data fitted by Hill´s (1) hyperbolic equation truncated at forces > 80 % of maximum. Fits to simulated data (grey line) gave a/P_0^*= 0.15; P_0^*/P_0=1.19. For experimental data (black line), see Fig. 1 of main paper. (B). Amrinone conditions simulated using same parameter values as in A but with 2 kT increase in free energy of state A_2. The simulated data (grey circles) superimposed on the experimental amrinone data from Fig. 1 (black circles). Lines represent fits of the Hill equation to experimental (black line) and simulated data (grey line; a/P_0^*= 0.16; P_0^*/P_0= 1.17), as described above.

important rate constants are illustrated in Supplementary Fig. 7A – B. These changes compared to the control conditions (again assuming that $k'_6 << k'_2$) give just as good fit to the change in the maximum shortening velocity and the shape of the force velocity relationship as

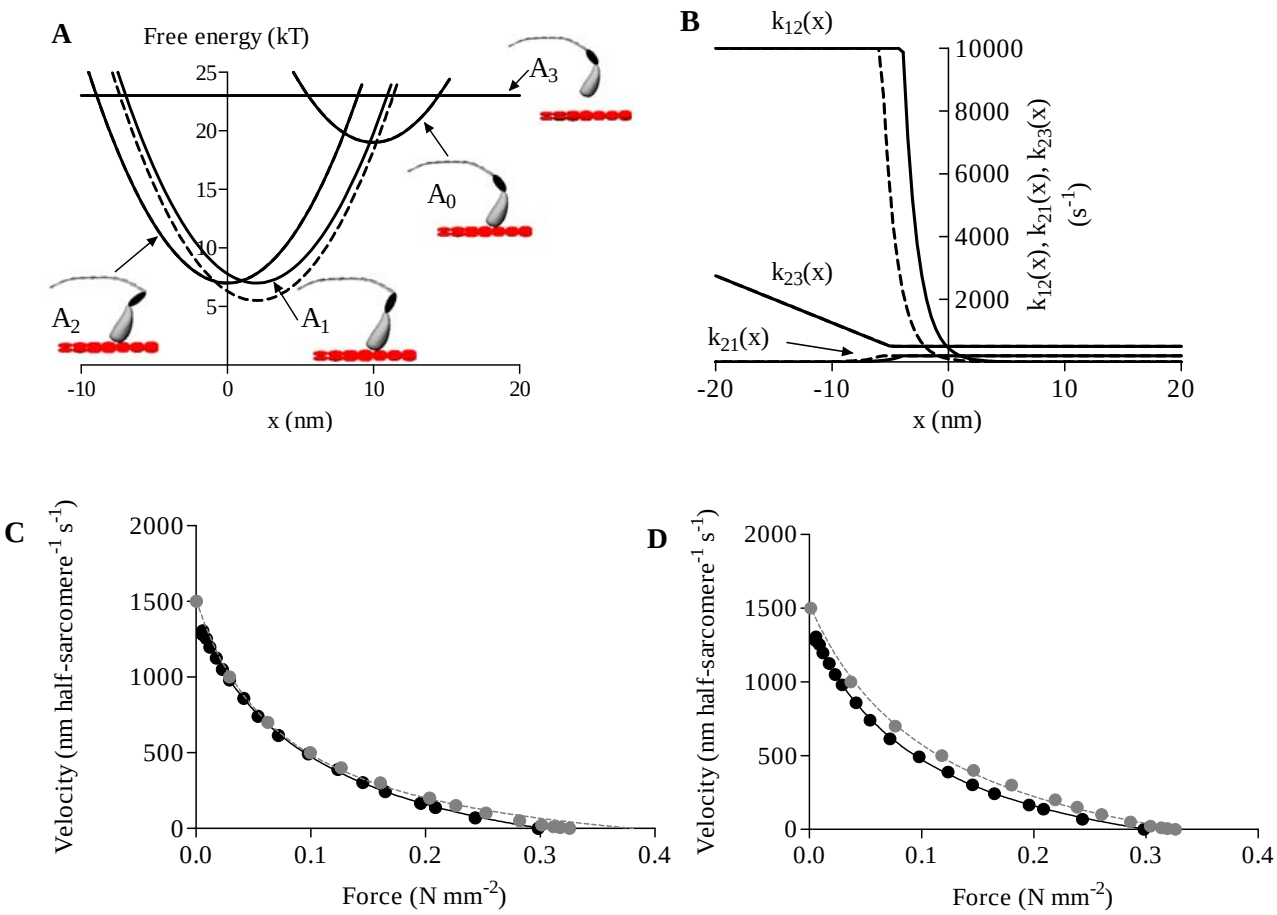

Supplementary Fig. 7. Simulation of amrione effects on basis of reduced free energy of state A_1. (A) The free energy diagrams for the control situation are illustrated by the full lines whereas the change assumed to be caused by amrinone is illustrated by the dashed line. The schematic drawings of the myosin head indicate differences in head configuration at the equilibrium positions (free-energy minima) of each state. (B) The amrinone-induced change in the free-energy of the state A_1 leads to the changes in the rate function $k_{12}(x)$ that governs the transition from A_1 to A_2 (filled line, control; dashed line, amrinone). Also the reverse rate constant $k_{21}(x)$ is changed at low x-value to be consistent with the free energy diagrams in A. However, amrinone did not affect the detachment rate function $k_{23}(x)$ since it was assumed that $k'_6 << k'_2$. (C) Amrinone conditions simulated by stabilization of the A_1 state by 1.5 kT without further changes. The simulated data (grey circles) are superimposed on the experimental amrinone data from Fig. 1 in main paper (black circles). Lines represent fits of the Hill equation to experimental (filled line) and simulated data (dashed grey line; $a/P_0^* = 0.204$; $P_0^*/P_0 = 1.174$), as described above. (D) Amrinone conditions (grey circles) simulated by stabilization of the AM*ADP (A_1) state by 1.5 kT (Suppl. Fig. 7 A) and increase of attachment rate function $k_{30}(x, v)$ by 33 % (compared to simulation in B) for large v. Black filled and grey dashed lines represent the Hill equation fitted to the experimental and simulated data ($a/P_0^* = 0.354$; $P_0^*/P_0 = 1.031$), respectively.

the assumption that the free energy of the state A_2 is increased. However, the simulated increase in the isometric force is considerably larger than observed experimentally. This effect, as well as the entire simulated force-velocity relationship, is illustrated in the Supplementary Fig. 7 C. As in the case with an increase in the free energy of state A_2 (Fig.

10, main paper) the additional assumption that amrinone increases the rate constant of cross-bridge attachment during shortening (but not in the isometric state) improves the reproduction of the amrinone induced changes in overall shape of the force-velocity relationship (Supplementary Fig. 7 D).

Relevant extracts from Simnon™ source code for the simulation of force-velocity data using the original model of Edman *et al.*(17)

Comments in italic below. Two communicating modules of the program are listed.

1) Rate functions and parameter values

continuous system parameters

```
"Communication with system" diffeq'2
input x v1
output kminus f fminus f2 f2minus kplus g k extd ext0 ext1 ext2

"Attachment rate constants and rate constants for reversal of attachment (k30 and k03
"in paper)
f00=if v1<c2 then (f0+sqrt(v1)*(f10-f0)/sqrt(c2)) else f10
diff=(x-(ext0-lage))
fv=f00*exp(akten/2-(k/2)*diff*diff/skal)
fm=fv/exp(akten-(k/2)*(x-ext0)*(x-ext0))
f=if (x>maxy) then 0 else if (x<miny) then 0 else fv
fminus=if (fm>fc) then fc else fm
"
"Rate constants A0-A1 (k10 and k01 in paper)
f2minus1=kmin
f2exp=exp(akten1-(k/2)*(2*(ext0-ext1)*x-ext0*ext0+ext1*ext1))
f2h=f2minus1*f2exp
kvot1=f2minus1/f2h
f2=if (f2h>fc) then fc else f2h
f2minus=if (f2>(fc-1)) then kvot1*f2 else f2minus1
"Rate constants A1-A2 (k21 and k12 in paper)
kminus1=kmin
kplusf=kminus1*exp(akten2-(k/2)*(2*(ext1-ext2)*x-ext1*ext1))
kvot2=kminus1/kplusf
kplus=if (kplusf>fc) then fc else kplusf
kminus=if (kplus>(fc-1)) then kvot2*kplus else kminus1


"Dissociation rate constants (k23 in paper)
g1l=gmax-((gmax-gt)/(bryt-bryt1))*(x-bryt1)
gl2=gmax+(c1*(brytc-x))
gh1=if (x>bryt1) then g1l else if (x<brytc) then gl2 else gmax
```

```
g=if (x>bryt) then gt else gh1
"
"free energy
G0=20+(styvhet/2)*(x-ext0)*(x-ext0)
G1=14+(styvhet/2)*(x-ext1)*(x-ext1)
G2=8+(styvhet/2)*(x-ext2)*(x-ext2)
G3=23
G01Bolz=exp(-(G1-G0))
G12Bolz=exp(-(G2-G1))
G30Bolz=exp(-(G0-G3))

"parameters:
k=styvhet
km:75
styvhet:0.4
c1:150
lage:0.5
fc:10000
maxy:20
miny:2
f10:21.5
f0:9
c2:225
skal:1.3
akten:3
akten1:6
akten2:6
extd=7
ext0=10
ext1=5
ext2=0
gt:60
kmin:200
gmax:205
bryt:5
bryt1:-2
brytc:-5
gexp:0.7
end
```

2) Solution to differential equations

continuous system diffeq

```
"Communication with system " parameters"
input kminus f fminus f2 f2minus kplus g k extd ext0 ext1 ext2
output x v1

"Definition of states, derivatives and independent variable
state d a0 a1 a2 i i0 i1 i2 sa0 s1 s2 atpas stif
der dd da0 da1 da2  di di0 di1 di2 dsa0 ds1 ds2 datpas dstif
time t
```

```
pa0=-(f*d-(fminus+f2)*a0+f2minus*a1)/v
pa1=-(f2*a0-(kplus+f2minus)*a1+kminus*a2)/v
pa2=-(kplus*a1-(kminus+g)*a2)/v
pd=-(g*a2+fminus*a0-f*d)/v
pi=a0*k*(x-ext0)+a1*k*(x-ext1)+a2*k*(x-ext2)
di0=a0*k*(x-ext0)
di1=a1*k*(x-ext1)
di2=a2*k*(x-ext2)
dsa0=a0
ds1=a1
ds2=a2
da0=-pa0
da1=-pa1
end
```

Supplementary References

1. Hill, A. V. (1938) *Proceedings of the Royal Society* **B 126.**, 136-195
2. Klinth, J., Arner, A., and Mansson, A. (2003) *J Muscle Res Cell Motil* **24**, 15-32
3. Hamalainen, N., and Pette, D. (1993) *J Histochem Cytochem* **41**, 733-743
4. Mansson, A., and Edman, K. A. P. (1985) *Acta Physiol Scand* **125**, 481-493
5. Mansson, A. (1989) *Biophys J* **56**, 429-433
6. Bottinelli, R., Cappelli, V., Morner, S. E., and Reggiani, C. (1993) *J Muscle Res Cell Motil* **14**, 110-120
7. Nyitrai, M., Rossi, R., Adamek, N., Pellegrino, M. A., Bottinelli, R., and Geeves, M. A. (2006) *J Mol Biology* **355**, 432-442
8. Homsher, E., Wang, F., and Sellers, J. R. (1992) *Am J Physiol* **262**, C714-723.
9. Murphy, C. T., Rock, R. S., and Spudich, J. A. (2001) *Nat Cell Biol* **3**, 311-315.
10. Sasaki, N., and Sutoh, K. (1998) *Adv Biophys* **35**, 1-24
11. Patterson, B., Ruppel, K. M., Wu, Y., and Spudich, J. A. (1997) *J Biol Chem* **272**, 27612-27617.
12. Suzuki, Y., Ohkura, R., Sugiura, S., Yasuda, R., Kinoshita, K., Jr., Tanokura, M., and Sutoh, K. (1997) *Biochem Biophys Res Commun* **234**, 701-706.
13. Balaz, M., Sundberg, M., Persson, M., Kvassman, J., and Månsson, A. (2007) *Biochemistry* **46**, 7233-7251
14. Jung, H. S., Komatsu, S., Ikebe, M., and Craig, R. (2008) *Mol Biol Cell* **19**, 3234-3242
15. Allingham, J. S., Smith, R., and Rayment, I. (2005) *Nat Struct Mol Biol* **12**, 378-379
16. Kovacs, M., Thirumurugan, K., Knight, P. J., and Sellers, J. R. (2007) *Proc Natl Acad Sci U S A* **104**, 9994-9999
17. Edman, K. A., Mansson, A., and Caputo, C. (1997) *J Physiol (Lond)* **503**, 141-156
18. Duke, T. A. (1999) *Proc Natl Acad Sci U S A* **96**, 2770-2775
19. Duke, T. (2000) *Philos Trans R Soc Lond B Biol Sci* **355**, 529-538
20. Pate, E., and Cooke, R. (1989) *J Muscle Res Cell Motil* **10**, 181-196.
21. Siemankowski, R. F., Wiseman, M. O., and White, H. D. (1985) *Proc Natl Acad Sci U S A* **82**, 658-662
22. Weiss, S., Rossi, R., Pellegrino, M. A., Bottinelli, R., and Geeves, M. A. (2001) *J Biol Chem* **276**, 45902-45908.